Biogeosciences
Discussions

A laboratory experiment of intact polar lipid degradation in sandy sediments

J. Logemann[1,*], J. Graue[1,*], J. Köster[1], B. Engelen[1], J. Rullkötter[1], and H. Cypionka[1]

[1]Institute for Chemistry and Biology of the Marine Environment (ICBM), Carl von Ossietzky University of Oldenburg, P.O. Box 2503, 26111 Oldenburg, Germany
[*]These authors contributed equally to this work.

Abstract

Intact polar lipids (IPLs) are considered biomarkers for living biomass. Their degradation in marine sediments, however, is poorly understood and complicates interpretation of their occurrence in geological samples. To investigate the turnover of IPLs, a degradation experiment with anoxic sandy sediments from the North Sea was conducted. Intact cells of two organisms that do not naturally occur in North Sea sediments were chosen as IPL sources: (i) *Saccharomyces cerevisiae*, representative for ester-bound acyl lipids that also occur in *Bacteria*, and (ii) the archaeon *Haloferax volcanii*, representative for ether-bound isoprenoid lipids. Surprisingly, IPLs with phosphoester-bound head groups showed approximately the same degradation rate as IPLs with glycosidic head groups. Furthermore, the results indicate a relatively fast degradation of *S. cerevisiae* IPLs with ester-bound moieties (analogs of bacterial membrane lipids) and no significant degradation of archaeal IPLs with ether-bound moieties. Pore water and 16S rRNA-based DGGE analysis showed only a minor influence of the IPL source on microbial metabolism and community profiles. Due to our results, the IPL-based quantification of *Archaea* and *Bacteria* should be interpreted with caution.

1 Introduction

Intact polar lipids (IPLs) have widely been used as biomarkers for living organisms in sediments and water columns for several years (e.g. Zink et al., 2003; Sturt et al., 2004; Biddle et al., 2006; Ertefai et al., 2008; Rossel et al., 2008). Additionally, IPLs are applied as chemotaxonomic markers as some of these molecules are representative for specific microbial clades. The chemotaxonomic information of IPLs is based on the combination of various head groups with different side chains that are attached to a glycerol backbone by two different bonding types. In general, bacterial and eukaryal cytoplasma membranes contain intact polar lipids with unbranched ester-bound fatty acid moieties. In contrast, archaeal IPLs contain ether-bound isoprenoid moieties.

This difference between bacterial and archaeal IPLs is used to quantify *Bacteria* and *Archaea* in sediments and water samples (e.g. Rossel et al., 2008). Thus, IPL analysis is valuable as an alternative or complementary technique to standard microbiological methods. On a higher chemotaxonomic level ammonia-oxidizing bacteria can be identified by the presence of ladderane lipids (Kuypers et al., 2003; Sinninghe Damsté et al., 2005). Intact polar lipids with mixed ether/ester-bound moieties attached to the glycerol backbone were found in some strains of sulfate-reducing bacteria (Rütters et al., 2001). Separate $\delta^{13}C$ analysis of polar head groups or unpolar core lipids of IPLs can also be used to gain information on the metabolism of their producers (Lin et al., 2010; Takano et al., 2010).

However, one fundamental assumption underlies most of these applications: Intact polar lipids are considered to degrade rapidly after cell death (White et al., 1979; Harvey et al., 1986). Harvey et al. (1986) examined the degradation of both, a glycosidic ether lipid and ester-bound phospholipids. Based on their findings the authors assumed that intact polar lipids with glycosidic head groups show a higher stability against degradation than intact polar lipids with phosphoester head groups. Based on the results of Harvey et al. (1986) modeling was used by Lipp et al. (2009) and Schouten et al. (2010) to assess the potential preservation of fossilized IPLs of planktonic origin during sediment burial.

The quantification of *Bacteria* and *Archaea* in the deep marine biosphere by IPL analysis and fluorescence in situ hybridization (FISH) in comparison to catalyzed reporter deposition fluorescence in situ hybridization (CARD-FISH) and quantitative polymerase chain reaction (q-PCR) analysis is controversially discussed in several studies (e.g. Biddle et al., 2006; Lipp et al., 2008). A reason for the contradictory abundances of *Archaea* and *Bacteria* in these studies may be that ether-bound archaeal IPLs are more stable than their ester-bound bacterial counterparts, which in turn may lead to an overestimation of archaeal cell numbers. However, the lack of a broad study on the degradation of intact polar lipids, which includes lipids with phosphoester and glycosidic bound head groups as well as ester and ether bound moieties, that occur in

3291

Bacteria and *Archaea* respectively, makes it necessary to revisit the degradation of IPLs to ensure the robustness of this proxy.

We designed a degradation experiment to answer three general questions: What are the degradation rates of IPLs? Are there differences between ester- and ether-bound intact polar lipids and what is the influence of the bonding type of the head group upon lipid degradation? How does the microbial community change over time and what are the main degradation products? The main degradation experiment was accompanied by two controls: The first control was intended to assess any processes that are not mediated by microorganisms and lead to the degradation of the added IPLs. This control is subsequently named "abiotic control". The second control was used to investigate the influence of the addition of inactive biomass on the microbial community and to monitor the development of the microbial community without any further substrate addition under laboratory conditions. This control is subsequently named "untreated control".

2 Material and methods

2.1 Experimental setup

The incubation vessels for the degradation experiment and the untreated control had a total volume of 2.5 l each and were filled with 3 kg wet sediment (water content 20 % wt). The sediment used in this experiment had been freshly collected in November 2009 on the Janssand, a tidal flat located approximately 3 km south of Spiekeroog island, North Sea, Germany (53°44.178′ N and 07°41.974′ E). For sampling, the top cm of the oxic surface sediment was removed until only black anoxic sediment was visible. The underlying sediment was transferred into plastic containers that were sealed by a lid, transported to the laboratory and stored at 4 °C for one week prior to further use. The total organic carbon (TOC) content was 0.23 %. It was calculated as the difference between total carbon (Vario EL Cube, Elementar Analysensysteme GmbH, Germany)

3292

and inorganic carbon (analyzed in a UIC CO_2 coulometer). A total of 2.5 g *Saccharomyces cerevisiae* biomass (elemental composition: 45.1 % C, 7.9 % H, 7.9 % N and 0.4 % S; % of dry mass) as source for ester-bound IPLs and 1.25 g of Haloferax volcanii (18.9 % C, 3.6 % H, 4.7 % N and 0.7 % S; % of dry mass) as source for ether-bound IPLs were added to the sediment in the incubation vessels used to study IPL degradation. The experimental parameters for the untreated control were the same as for the degradation experiment but no inactive cell material was added. To prevent contamination with microorganisms due to frequent sampling in the abiotic control, 100 ml bottles instead of one 2.5 l incubation vessel were used. The bottles contained 50 g of sediment, 50 mg, dry mass inactive biomass of *S. cerevisiae* and 25 mg, dry mass inactive H. volcanii biomass and were closed with rubber stoppers. The incubation vessels of the abiotic control were autoclaved after addition of the intact polar lipid containing cell material.

2.2 Source material for intact polar lipids

As source for intact polar lipids two different organisms were used which do not occur in the North Sea sediment. As source for ether-derived IPLs a pure culture of Haloferax volcanii (DSM No. 16227) was grown at 37 °C in "Haloferax sulfurifontis medium" (DSMZ No. 1018). This archaeon provided two kinds of structurally different molecules – first, two IPLs with ether-bound isoprenoid moieties (PGP-Me, PG; Fig. 1) and a phosphoester head group and second, one IPL with ether-bound isoprenoid moieties and a glycosidic head group (S-GL-1; Fig. 1). The cells were harvested at the end of the exponential growths phase. None of the H. volcanii IPLs occur in the natural sediment and thus all of them could be used as tracers to monitor the degradation of ether-bound IPLs. Commercially available *Saccharomyces cerevisiae* (baker's yeast; Fala GmbH, Germany) was used as source for IPLs with ester-bound acylic moieties and phosphoester head groups. *S. cerevisiae* cells harbour a broad variety of IPLs which were partly used as tracers because these IPLs were not synthetized by the natural sediment microbial community. The *S. cerevisiae* and the harvested

archaeal cells were freeze dried and stored at −20 °C. Before use in the experiment, H. volcanii and *S. cerevisiae* cells were pasteurized at 100 °C for 30 min. Thereafter, part of the cells was transferred to fresh medium ("Haloferax sulfurifontis medium" and yeast extract medium, respectively) and analyzed for growth to exclude that the cells are still alive and able to grow. Identification of *S. cerevisiae* lipids was achieved by HPLC-MS/MS experiments and by comparison to commercially available standards. The lipids of H. volcanii were identified by MS/MS experiments and comparison with published results of lipid structures (Sprott et al., 2003). In this experiment we monitored the concentrations of 16 intact polar lipids −13 ester-bound and 3 ether-bound ones.

2.3 Incubation parameters and sampling

After starting the experiment, the incubation vessels were stored at room temperature in the dark. Before sampling, the sediment was homogenized for a minimum of 20 min on a mixing device. Head-space gas samples were taken with a syringe directly before sampling the sediment. For sediment and pore water sampling, the incubation vessels were transferred into a glove box with an oxygen-free nitrogen (99 %) and hydrogen (1 %) atmosphere. Samples were taken as triplicates, aliquots of 8–12 g sediment for IPL analysis and 3–5 g sediment for RNA extraction. Pore water (1–2 ml) was extracted with rhizones (Rhizon CSS 5 cm, Rhizosphere Research Products, Wageningen, the Netherlands) from the samples that were collected for IPL analysis. Previous investigations had ensured the absence of IPLs in the pore water samples. Until further processing, all samples were stored at −20 °C. The samples for RNA extraction were kept at −80 °C. After sampling, the head space of the incubation vessels was flushed with nitrogen to remove traces of hydrogen that was used in the glove box to sustain the oxygen-free atmosphere.

2.4 Lipid extraction

The wet sediments were extracted using a modified Bligh & Dyer method according to Sturt et al. (2004). In the first three extraction steps, a single-phase mixture of methanol, dichloromethane and phosphate buffer (2:1:0.8, v/v/v) was used. In the following three extraction steps, trichloroacetic acid was used instead of phosphate buffer. The combined extracts were collected in a separatory funnel. Phase separation was achieved by addition of dichloromethane and water to a final mixture of 1:1:0.9 (v/v/v, methanol, dichloromethane, aqueous phase). The organic phase containing the IPLs was removed and the aqueous phase was washed three times with dichloromethane. The dry extracts were stored in a freezer at $-20\,^{\circ}$C until further use.

2.5 HPLC-MS

Intact polar lipids were analyzed by HPLC (2695 separation module, Waters, Milfort, USA) coupled to a time-of-flight mass spectrometer equipped with an electrospray source (Micromass, Q TOF micro, Waters, Milfort, USA). HPLC separation was achieved on a diol phase (Lichrospher100 Diol 5 µ, CS – Chromatographie Service, Langerwehe, Germany) using a 2×125 mm column. A flow rate of $0.35\,\mathrm{ml\,min^{-1}}$ was employed with the following solvent gradient: 1 min 100 % A, increasing over 20 min to 35 % A, 65 % B using a concave curvature, followed by 40 min of reconditioning (Rütters et al., 2001). Eluent A was a mixture of n-hexane, i-propanol, formic acid and a solution of 25 % ammonia in water (79:20:1.2:0.04 by volume), eluent B was ipropanol, water, formic acid and a solution of 25 % ammonia in water (88:10:1.2:0.04 by volume). After addition of an injection standard (O-PE, phosphatidyl ethanolamine diether with two C_{16} acyl moieties), the extracts were dissolved in the starting eluent and directly analyzed. In this study, we exclusively report the change of those compounds that were added with the inactive cell material and did not occur in the natural sediment. Due to the lack of analytical standards for the archaeal glycolipids used, it was not possible to determine the absolute concentrations of these compounds. Instead, ratios of

3295

peak areas of the monitored compounds to the peak area of the injection standard for each sample were calculated. Subsequently, the calculated values are named relative concentrations. Since all samples had the same matrix background, this procedure should give reasonable results without any influence of changing ionization. The analytical error varied between 0.5 and 7 % depending on the investigated IPL and was determined by repeated analysis of the same samples taken at three different times. The limit of detection in general depends on the ionization efficiency for every analyzed compound and typically lies between 2–10 ng per injection and IPL for the used mass spectrometer (Micromass Q-TOF micro, Waters, Milfort, USA).

2.6 Chemical analyses of microbial metabolites

Concentrations of fermentation products in the pore water were analyzed by high-performance liquid chromatography (Sykam, Fürstenfeldbruck, Germany) using an Aminex HPX-87H column (Biorad, München, Germany) at $60\,^{\circ}$C. The eluent was $5\,\mathrm{mM\,H_2SO_4}$ at $0.5\,\mathrm{ml\,min^{-1}}$. Organic acids were detected by an UV-VIS detector (UVIS 204; Linear Instruments, Reno, USA) at 210 nm. Alcohols were detected by a refractive-index detector (Knauer, Berlin, Germany). Prior to injection, the pore water was filtered through a 2 µm filter. Sulfate concentrations were measured by an ion chromatograph (Sykam, Fürstenfeldbruck, Germany) with an anion separation column (LCA A24; Sykam, Fürstenfeldbruck, Germany) at $60\,^{\circ}$C followed by conductivity detection. The eluent consisted of 0.64 g sodium carbonate, 0.2 g sodium hydroxide, 150 ml ethanol and 2 ml modifier (0.1 g 4-hydroxybenzonitrile/10 ml methanol) filled up to 1 l with distilled water. The flow rate was set to $1.2\,\mathrm{ml\,min^{-1}}$. Prior to analysis the samples were 1 to 100 diluted in eluent without modifier. The concentrations of gaseous compounds were determined by an 8610C gas chromatograph (Schambeck SFD GmbH, Honnef, Germany). Analysis was carried out with argon (1 ml/min) as carrier gas and at a column oven temperature of $40\,^{\circ}$C. For analysis of molecular hydrogen and methane a molecular sieve 13X packed column was used, whereas carbon dioxide was separated by a HayeSep D packed column. A thermal conductivity detector ($256\,^{\circ}$C) and a

3296

flame ionization detector (380 °C) were connected in series for detection of the gases. Sulfide concentrations were determined photometrically as described by Cord-Ruwisch et al. (1985). The pH was adjusted at each sampling point to values between 7 and 7.5 by addition of hydrochloric acid. Hydrogen sulfide was expelled by flushing the headspace with CO_2. After each CO_2 flushing the headspace was replaced with N_2.

2.7 Determination of total cell numbers

Total cell counts were obtained after SYBR Green I staining according to a protocol of Lunau et al. (2005), which was adapted to sediment samples. For sample fixation, $0.5\,cm^3$ of sediment was transferred to 4.5 ml of fixing solution (63 ml distilled water, 30 ml methanol, 2 ml of 25 % aqueous glutardialdehyde solution, 5 ml Tween 80) and incubated at room temperature overnight. For detaching cells from particles, the sediment slurries were incubated for 15 min at 35 °C in an ultrasonic bath (35 kHz, 2×320 W per period; Sonorex RK 103 H, Bandelin, Mörfelden-Walldorf, Germany). Homogenized aliquots of 20 µl were equally dispensed on a clean microscope slide in a square of 20×20 mm. The slide was dried on a heating plate at 40 °C. A drop of 12 µl staining solution (190 µl Moviol, 5 µl SYBR Green I, 5 µl 1 M ascorbic acid in TAE buffer) was placed in the center of a 20×20 mm coverslip, which was then placed on the sediment sample. After 10 min of incubation, 20 randomly selected fields or at least 400 cells were counted for each sediment sample by epifluorescence microscopy.

2.8 RNA extraction and quantification

Total RNA was extracted from 1 g sediment using the AllPrep DNA/RNA Mini Kit (Qiagen, Hilden, Germany) according to the manufacturer's instructions. For cell disruption, 1 g sediment and 1 ml RLT Buffer were added to 1 g glass beads (0.18 mm diameter, Sartorius, Göttingen, Germany). Samples were homogenized for 90 s using a Mini Beadbeater (Biospec Products, Bartlesville, USA). For quantification, 100 µl of Ribo-Green (Invitrogen, Eugene, USA) solution (diluted 1:200 in TE buffer; pH 7.5) were

added to 100 µl of RNA extract (each sample diluted 1:100 in TE buffer; pH 7.5) and transferred to a microtiter plate. Serial dilutions ($200\,ng\,µl^{-1}$ to $1\,ng\,µl^{-1}$) of E. coli 16S and 23S ribosomal-RNA (Roche, Grenzach-Wyhlen, Germany) were treated as described above and served as a calibration standard in each quantification assay. Fluorescence was measured at an excitation of 485 nm and an emission of 520 nm.

2.9 Quantitative reverse transcription PCR (qRT-PCR)

Bacterial and archaeal 16S rRNA gene copy numbers were determined by quantitative reverse-transcription PCR using the OneStep RT-PCR Kit (Qiagen, Hilden, Germany). The primer pairs 519f/907r and s D Arch 0025-a-S-17/s-D-Arch-0344-a-S-20 were used to quantify bacterial and archaeal RNA, respectively. Primer sequences for these two domains are given in Wilms et al. (2007). Each 25 mul PCR reaction contained 15.9 µl nuclease-free water, 5× RT-PCR Buffer (Qiagen, Hilden, Germany), 0.4 mM dNTP Mix (Qiagen, Hilden, Germany), 0.2 µM of each primer, 0.1 µl of a 1 to 500 diluted SYBR Green I solution (Molecular Probes, Eugene, OR, USA), 1 µl One Step Enzyme Mix (Qiagen, Hilden, Germany) and 1 µl standard (10^9 to 10^2 gene copies per µl) or environmental target RNA. Thermal cycling comprised a reverse transcription step for 30 min at 50 °C, followed by an initial denaturation step for 15 min at 95 °C, 40 cycles of amplification (10 s at 94 °C, 20 s at 54 °C for bacterial RNA quantification or 48 °C for archaeal RNA quantification, 30 s at 72 °C and 20 s at 82 °C) and a terminal step (2 min at 50 °C). After each run, a melting curve was recorded between 50 °C and 99 °C to ensure that only specific amplification had occurred. 16S and 23S ribosomal RNA of E. coli (Roche Diagnostics GmbH, Grenzach-Wyhlen, Germany) served as standard for bacterial gene targets. A PCR product was used as standard for quantification of Archaea. Archaeal primer sequences and PCR conditions are given in Wilms et al. (2007). For each amplification the OneStep RT-PCR Kit was used according to the manufacturer's instructions. All PCRs contained a reverse transcription step (30 min, 50 °C) prior to amplification.

2.10 Denaturing gradient gel electrophoresis (DGGE) analysis

Partial 16S rRNA were amplified using the OneStep RT-PCR Kit (Qiagen, Hilden, Germany) with bacterial primers GC-357f and 907r as given in Muyer et al. (1995) and archaeal primers S D Arch-GC-0344-a-S-20 und 907r as described previously (Wilms et al., 2006). Each forward primer contained a GC-clamp (Muyzer et al., 1993). Thermal cycling included a reverse transcription step for 30 min at 50 °C, followed by an initial denaturation step for 15 min at 95 °C, 30 cycles of bacterial RNA amplification and 35 cycles of archaeal RNA amplification (30 s at 94 °C, 45 s at 57 °C for bacterial RNA amplification or 48 °C for archaeal RNA amplification, 60 s at 72 °C), and a terminal step (10 min at 72 °C). The PCR amplicons and loading buffer (40% [wt/vol] glycerol, 60% [wt/vol] 1× tris acetate-EDTA [TAE], and bromphenol blue) were mixed in a ratio of 1:2. DGGE was carried out as described by Süß et al. (2004) using an INGENYphorU-2 system (Ingeny, Leiden, Netherlands) and a 6% (wt/vol) polyacrylamide gel containing denaturant gradients of 50 to 70% for separation of bacterial PCR products. For separation of archaeal PCR products a denaturant gradient of 30 to 80% was prepared. The gels were stained for 2 h with 1× SYBR Gold (Molecular Probes, Leiden, Netherlands) in 1× tris-acetate-EDTA buffer and washed for 20 min in distilled water prior to UV transillumination.

2.11 Sequence analysis

DGGE bands were excised for sequencing and treated as described by Del Panno et al. (2005) without the second denaturing gel for purification. For reamplification the same primers pairs as described above were used without the GC-clamp. The bacterial reamplification comprised 26 PCR cycles (annealing temperature 55 °C) whereas the archaeal reamplification comprised 32 cycles (annealing temperature 48 °C). For subsequent sequence analysis, PCR products of DGGE bands were purified using the QIAquick PCR purification kit (Qiagen, Hilden, Germany) and commercially sequenced by GATC Biotech (Konstanz, Germany). The partial 16S rRNA sequences of the DGGE bands were compared to those in GenBank using the BLAST function (Altschul et al.,

1997). Accession numbers of all partial 16S rRNA gene sequences obtained in this study will be added to the EMBL database upon acceptance of the manuscript.

3 Results

The monitored microbial processes demonstrated similar trends in the degradation experiment and the untreated control. In contrast, the abiotic control showed no sign of sulfate reduction, methanogenesis, IPL degradation, fermentation or any other microbial activity as demonstrated by the stability of all measured parameters (data not shown). This indicates that the degradation of IPLs was exclusively mediated by microorganisms.

3.1 Sulfate and methane data

Sulfate and methane are part of the terminal mineralization processes and their concentrations were monitored to assess the current status of the experiment. Sulfate was completely consumed within the first 9 days (Fig. 2). Between day 9 and day 20, the sulfate concentration remained below the detection limit, until sulfate was refilled. Sulfate was replenished to mimic the natural environment. At the end of the experiment, sulfate was consumed more slowly than at the beginning, indicating the depletion of electron donors. The sulfate concentration decreased to 9 mM at day 97. Large amounts of methane were only detected in the absence of sulfate. The reason for this is, that methanogens commonly use the electron donors also used by sulfate-reducing bacteria. Since sulfate reduction is energetically favored methanogenesis is suppressed in the presence of sulfate (Oremland and Taylor, 1977). Gaseous sulfide (produced by sulfate reduction) was removed from the headspace during every sampling by purging with nitrogen. The concentration of dissolved sulfide in the pore water remained relatively low until day 27 (6 mM). The maximum concentration was reached at day 76 (38 mM). Since this is a toxic concentration for most microorganisms, the headspace

was purged with CO_2 to release the hydrogen sulfide. After flushing, the CO_2 in the head space was replaced with N_2. The pH increased constantly in the degradation experiment and the untreated control and was adjusted to values between pH 7 and 8 by addition of hydrogen chloride. Oxygen was never detected in any incubation vessel.

3.2 Degradation of intact polar lipids

The relative concentrations of ester-bound IPLs decreased in the course of the experiment whereas the relative concentrations of ether-bound IPLs remained stable. The head groups had no significant influence on the observed degradation pattern. The relative concentrations of ester-bound IPLs with PC and PI head groups showed no significant change in the first days of the degradation experiment. Beginning at day 5, they decreased rapidly over 5 days followed by a phase of moderate loss until day 90. In case of PE and PS (Fig. 3c and d) higher relative concentrations were found at day 5. In the following period the signal decreased over the rest of the experiment.

In contrast to this, the relative concentrations of all ether-bound IPLs (Fig. 4) scattered but did not decrease significantly until the end of the degradation experiment. The relative concentrations of ester- and ether-bound IPLs in the abiotic control showed a slight decrease relative to day 0 in the course of the experiment (Fig. 5). The small decrease in the abiotic control at day 1 was probably caused by inhomogeneity since the drop occurred in both ester- and ether-bound IPL quantifications.

3.3 Intact polar lipids in the untreated control

Samples from the untreated control were taken in the same sampling intervals as in the degradation experiment. Most of the IPLs added to monitor the degradation were not detected in the untreated control. Exceptions were the IPLs PE 34:2 and PE 36:2, but compared to the corresponding PEs in the added biomass their total amount was low (less than 3 %). However, other IPLs such as SQDG (sulfoquinovosyl diacylglycerol) and ester-bound PG were identified in the untreated control. Additionally, ester-bound PEs with side chains different from those in the degradation experiment were found

(31:0, 31:1, 33:1, 33:2, 35:2). SQDG was the most prominent IPL in the untreated control. It showed increasing abundances from day 0 to day 23 and then a decrease to the starting value at a moderate rate after a major drop between days 23 and 27. PE and PG showed an increase between day 0 and day 5 and returned to the starting values in the course of the experiment.

3.4 Microbial fermentation

Fermentation products were analyzed to monitor the utilization of organic matter. The data show the net balance of fermentation products since they are produced and consumed simultaneously (Fig. 6). In the beginning of the experiment the short-chain fatty acids were produced faster than consumed as indicated by their increasing concentrations. The main fermentation product was acetate followed by propionate, butyrate and valerate. During the final phase of the experiment, the fermentation products were utilized at the same rate as they were produced or the consumption was faster than the formation. Ethanol was also produced but could not be quantified due to signal overlapping with those of other unknown organic compounds from the sediment matrix. The graphs for short-chain fatty acids in the degradation experiment and the untreated control shared the same characteristics. The accumulation of short-chain fatty acids tended to be slightly faster in the degradation experiment but overall the added cell material had only a minor influence on the shape of the production curves of short-chain fatty acids. This indicates that the experiment was not disturbed by the addition of biomass as external substrate.

3.5 Succession in microbial abundance, diversity and activity

The development of the microbial communities was monitored to obtain background information for the degradation of IPLs. The total cell counts of the degradation experiment and the untreated sediment showed the same trend and decreased only slightly during the experiment (Fig. 7). The total cell numbers of the degradation experiment

were marginally higher than those of the untreated control. The numbers of bacterial 16S rRNA targets were one to two orders of magnitude higher than those of Archaea. Between day 7 and day 16, the bacterial 16S rRNA copy numbers dropped significantly and returned to their previous values. The number of archaeal 16S rRNA copies showed a generally increasing trend. After day 20, both the number of bacterial and archaeal 16S rRNA targets remained relatively constant. The RNA content of the sediment ranged from 80 to 4800 ng cm^{-3}. Ravenschlag et al. (2000) determined a rRNA content of 0.9 to 1.4 fg rRNA per cell for two sulfate-reducing bacteria from surface sediments. Using these values to assess the total cell numbers for our study, the calculated values range between 8.9×10^7 to 3.4×10^9 cells cm^{-3}, which fits nicely to our total cell counts. The community profiles of the degradation experiment and the untreated sediment looked similar to each other. Initially, the community structure was highly diverse. This diversity decreased in the course of the experiment probably due to a diminishing substrate spectrum as indicated in Fig. 6. Sequencing of representative bands indicated the presence of different fermenting and sulfate-reducing bacteria. The most conspicuous organisms were relatives of *Pelobacter* sp. and *Dethiosulfovibrio acidaminovorans*. These bacteria were highly abundant during the end phase of the experiment, when acetate and propionate were absent, indicating an enhanced activity in this period. A sequence of a *Cytophaga fermentans*-related organism was detected after one week, also hinting toward an increased activity of that organism from that time on. Additionally, this bacterium showed a higher abundance in samples from the degradation experiment. The abundance of other organisms, most of them being sulfate-reducing bacteria like a *Desulfobacter psychrotolerans*-related organism, appeared to be relatively constant over time, since sulfate was available almost during the entire experiment. Sulfur-oxidizing bacteria were only detected at the beginning of the experiment. Sequences affiliated to diatom chloroplasts were found during the complete course of the experiment.

The archaeal community pattern showed minor differences between the degradation experiment and the untreated control (Fig. 9). A *H. volcanii* could only be detected

at the very first sampling point in the degradation experiment. This indicated that the *H. volcanii* cells were successfully disintegrated during the experiment.

For both, the degradation experiment and the untreated control six bands were detected throughout the whole experiment. All sequences were closely related to two different organisms, either *Methanogenium frigidum* or *Methanogenium marinum*. The community patterns reflect the quantification of Archaea by qPCR: In the first week when the number of archaeal 16s rRNA gene targets was lowest, only very faint bands were detected in the DGGE profile. In the beginning of the experiment, when sulfate was still present, no methanogenic archaea could be detected (Fig. 9). Only after depletion of sulfate the rRNA of methanogens was found. The presence and activity of these organisms were supported by the methane production that was observed in the absence of sulfate. In all samples, the content of eukaryotic RNA was too low to obtain sufficient PCR-products to prepare a DGGE with eukaryotic primers.

3.6 Total organic carbon

The carbon content was analyzed at five time points of the degradation experiment and the untreated control. The difference in organic matter between the degradation experiment and the untreated control reflected the amount of organic carbon that was added to the degradation experiment with the inactive cell material of *S. cerevisiae* and *H. volcanii*. Although we added 1.36 g of cell-derived organic carbon which increased the TOC content of the natural sediment (0.22% Corg) by roughly 25%, no pronounced difference was visible between the degradation experiment and the untreated control for all other parameters.

3.7 Effects of sediment-derived organic carbon on microbial processes

The increasing concentrations for fermentation products and total cell counts within the first week demonstrate a stimulation of microbial activity. This was likely caused by a temperature increase from 4 °C (storage temperature) to 20 °C in the laboratory. The addition of biomass caused a faster increase for methanogenesis and fermentation.

The added biomass also resulted in slightly increased values for sulfate consumption, methane production and fermentation (Figs. 2 and 6). The absolute amount of IPLs that were added with the biomass of *H. volcanii* and *S. cerevisiae* was low compared to other organic compounds present in the sediment itself. Therefore, the fermentation products do not only reflect the products of IPL degradation but mainly the degradation products of the organic matter which originated from the natural sediment.

4   Discussion

In this experiment ester-bound bacteria-like IPLs were faster degraded than ether-bound archaeal IPLs. The bonding type of the head group had no influence on the degradation rate.

4.1   Assessment of experimental conditions

On the first view the scattering for ether-bound IPLs appears to be much higher than for ester-bound IPLs. This different behavior is an artifact of the data processing applied. To monitor the degradation of IPLs the relative concentration for each monitored IPL was calculated. With this method, a scattering of IPL signals with values near the detection limit becomes much less visible than the scattering of IPL signals with values in the range of the injection standard. This explains the smooth degradation curve for ester-bound IPLs in Fig. 3 after the first 10 days. Nevertheless, these analytical limitations do not have any impact on the general results of this study.

Haloferax volcanii and *Saccharomyces cerevisiae* do not naturally occur in tidal flat sediments. Thus it could be assumed that the observed degradation rates of IPLs could be different from those originating from the natural community. However, the source of the ether-bound and ester-bound IPL should have no influence on the degradation rate since the chemical structure and the bonding types of the added material can also be found in IPLs that naturally occur in Wadden Sea sediments (Rütters et al., 2001).

One could argue that the different degradation pattern observed for ether- and ester-bound IPLs are caused by a selective protection of ether-bound IPLs in intact *H. volcanii* cell material and on the other hand disrupted cells of *S. cerevisiae*. This is unlikely because the rRNA of *H. volcanii* related archaea was only found at the very beginning of the experiment. Additionally, cultivation attempts with pasteurized cells showed no growth which indicates that the *H. volcanii* cells were killed during the experiment.

As displayed in Fig. 4, the results of ether-bound IPL analysis showed a non-systematic scattering. Adsorption/desorption processes of IPLs to/from the sediment matrix may be an issue. Sediment inhomogeneity is also a possible explanation. We tried to minimize this effect by the design of the incubation vessel and intense mixing on a mixing device prior to every sampling. In addition to this, directly before opening the incubation vessels in the anaerobic chamber, the sediment was resuspended by shaking. Other reasons for scattering IPL values may be varying extraction efficiencies or changing matrix effects during ESI-ionization which may add some scattering in addition to inhomogeneity.

4.2   Influence of bonding types and moieties on IPL degradation

The degradation pattern and hence the stability of all investigated ester-bound bacterial-like IPLs was approximately the same (Fig. 3a–d). It can be assumed that the degradation of ester-bound intact polar lipids was independent from the type of head group, since the core structures of these IPLs are generally the same. A similar behavior was observed for the ether-bound archaeal IPLs. But in contrast to the ester-bound bacterial IPLs, the investigated archaeal IPLs had two structurally different types of head groups – one glycosidic (S-GL-1) and two phosphoester (PG-Ar and PGP-Me; Fig. 1) head groups. Based on the study of Harvey et al. (1986) glycosidic ether lipids are commonly assumed to be more stable than phospholipids with ester-bound moieties. However, Harvey and coauthors investigated the degradation of a glycosidic ether lipid and a phosphoester lipid. They found a higher stability of the glycosidic ether lipid. In general, compared to glycosidic bonds phosphoester bonds

are chemically more labile. In combination with the findings of Harvey and coworkers this could lead to the assumption that the bonding type of the head group has a major influence on the IPL degradation rate. But in fact the study of Harvey et al. 1986 is not suitable to answer the question which part of an IPL-molecule (head group or moiety bonding type) is responsible for the observed differential stability of bacterial and archaeal IPLs. According to our results, we assume that the differences in chemical stability of IPLs play only a minor role during the degradation of IPLs, at least in the investigated system. Since the head groups had no influence on the IPL degradation rates the structurally different core lipids are assumed to cause the observed degradation rates.

In general complex molecules like lipids and proteins are hydrolyzed by exo- or ectoenzymes which are released by prokaryotic cells. Therefore, we conclude that microbiological enzymatic processes are the driving force in IPL degradation rather than expected chemical stabilities alone.

4.3 Microbial activity

Originally, the experiment was planned as an enrichment culture for lipid-degrading bacteria. It turned out, however, that the added cell material had only little influence on the community structure and the metabolic activity. This had a positive side-effect, since the processes which originally occur in tidal flat sediments were not disturbed and superposed. As a consequence the selected set-up is suitable to reflect the natural IPL degradation in such sediments.

Most of the *Archaea* in sediments are known to be methanogens (Wilms et al., 2007) or nitrifying archaea (Wuchter et al., 2007). They have a narrow substrate spectrum limited to simple molecules and are not known to degrade lipids. Probably, the main lipid degraders are *Bacteria* which are more abundant than *Archaea* in surface sediments (e.g. Beck et al., 2011).

Chloroplast RNA of diatoms was found throughout the whole course of the experiment. Since no oxygen and no light for algal growth were available in the experiment,

the diatoms might be inactive in a resting state. The RNA of chloroplasts is exceptionally stable, because the RNA in this cell organelle is surrounded by four membranes (Kroth and Strotmann, 1999). Another reason for the stability of chloroplast RNA may be that the diatoms were in fact active and survived by a heterotrophic kind of metabolism. Facultative heterotrophy is known for many diatoms, including several *Navicula* species (Lewin, 1953; Sherr and Sherr, 2007). Heterotrophically growing diatoms continue to synthesize their photosynthetic pigments in the dark and return immediately to photosynthesis under light exposure (Lewin and Hellebus, 1970). This indicates that chloroplast RNA is present even if no light is available.

The question if ester-bound lipids are recycled and used for membrane synthesis by *Bacteria* cannot be answered by our experimental-setup. However, enzymes are described for *Eukarya* and *Prokarya* that facilitate bidirectional ATP-independent flipping of polar lipids across cytoplasmic membranes (Sanyal and Menon, 2009). The incorporation of extrinsic cell building blocks is energetically useful for microorganisms because it is more efficient to recycle existing molecules than breaking them down to smaller molecules to synthesize them "de-novo". Takano and coworkers (2010) added ^{13}C labeled glucose to marine sediment and found that the ^{13}C was incorporated into the glycerol backbone of archaeal membrane lipids whereas the isoprenoid core lipids remained unlabeled. This indicates a recycling of comparable large membrane building blocks. To answer the question if IPLs can be recycled as intact molecules, stable-isotope probing (SIP) or ^{14}C-labeling would be suitable tools to follow the degradation and incorporation of IPLs and their resulting products.

5 Conclusions

The quantification of *Bacteria* and *Archaea* in the deep marine biosphere by IPL and FISH analysis led to the assumption that this habitat is dominated by *Archaea* (Biddle et al., 2006; Lipp et al., 2008). In contrast, catalyzed reporter deposition fluorescence in situ hybridization (CARD-FISH) and quantitative polymerase chain reaction (q-PCR)

suggest a predominance of *Bacteria* (Schippers et al., 2005; Inagaki et al., 2006). Our experiment shows that these interpretations have to be considered with caution, since ether-bound archaeal IPLs were clearly more stable than ester-bound bacteria-like IPLs over a period of 100 days. In nature, ether-bound IPLs may even be preserved for longer time periods since the enhanced temperature in the laboratory accelerated the degradation processes. Therefore IPL based quantification may lead to an overestimation of archaeal cell numbers.

References

Altschul, S. F., Madden, T. L., Schäffer, A. A., Zhang, J., Zhang, Z., Miller, W., and Lipman, D. J.: Gapped BLAST and PSI-BLAST: a new generation of protein database search programs, Nucleic Acids Res., 25, 3389–3402, doi:10.1093/nar/25.17.3389, 1997.

Beck, M., Riedel, T., Graue, J., Köster, J., Kowalski, N., Wu, C. S., Wegener, G., Lipsewers, Y., Freund, H., Böttcher, M. E., Brumsack, H.-J., Cypionka, H., Rullkötter, J., and Engelen, B.: Imprint of past and present environmental conditions on microbiology and biogeochemistry of coastal Quaternary sediments, Biogeosciences, 8, 55–68, doi:10.5194/bg-8-55-2011, 2011.

Biddle, J. F., Lipp, J. S., Lever, M. A., Lloyd, K. G., Sørensen, K. B., Anderson, R., Fredricks, H. F., Elvert, M., Kelly, T. J., Schrag, D. P., Sogin, M. L., Brenchley, J. E., Teske, A., House, C. H., and Hinrichs, K. U.: Heterotrophic archaea dominate sedimentary subsurface ecosystems off Peru, Proc. Natl. Acad. Sci. U.S.A., 103, 3846–3851, 2006.

Cord-Ruwisch, R.: A quick method for the determination of dissolved and precipitated sulfides in cultures of sulfate-reducing bacteria, J. Microbiol. Meth., 4, 33–36, 1985.

Del Panno, M. T., Morelli, I. S., Engelen, B., Berthe-Corti, L., Effect of petrochemical sludge concentrations on microbial communities during soil bioremediation, FEMS Microbiol. Eco., 53, 305–316, doi:10.1016/j.femsec.2005.01.014, 2005.

Ertefai, T. F., Fisher, M. C., Fredricks, H. F., Lipp, J. S., Pearson, A., Birgel, D., Udert, K. M., Cavanaugh, C. M., Gschwend, P. M., and Hinrichs, K. U.: Vertical distribution of microbial lipids and functional genes in chemically distinct layers of a highly polluted meromictic lake, Org. Geochem., 39, 1572–1588, 2008.

Harvey, H. R., Fallon, R. D., and Patton, J. S.: The effect of organic-matter and oxygen on the degradation of bacterial membrane lipids in marine sediments, Geochim. Cosmochim. Ac., 50, 795–804, 1986.

Inagaki, F., Nunoura, T., Nakagawa, S., Teske, A., Lever, M., Lauer, A., Suzuki, M., Takai, K., Delwiche, M., Colwell, F. S., Nealson, K. H., Horikoshi, K., D'Hondt, S., and Jørgensen, B. B.: Biogeographical distribution and diversity of microbes in methane hydrate-bearing deep marine sediments on the Pacific Ocean Margin, Proc. Natl. Acad. Sci. U.S.A., 103, 2815–2820, doi:10.1073/pnas.0511033103, 2006.

Kroth, P. and Strotmann, H.: Diatom plastids: Secondary endocytobiosis, plastid genome and protein import, Physiol. Plantarum, 107, 136–141, 1999.

Kuypers, M. M. M., Sliekers, A. O., Lavik, G., Schmid, M., Jørgensen, B. B., Kuenen, J. G., Damste, J. S. S., Strous, M., and Jetten, M. S. M.: Anaerobic ammonium oxidation by anammox bacteria in the Black Sea, Nature, 422, 608–611, 2003.

Lewin, J. C.: Heterotrophy in diatoms, J. Gen. Microbiol., 9, 305–313, 1953.

Lewin, J. and Hellebus, J.: Heterotophic nutrition of marine pennate diatom, Cylindrotheca fusiformis, Can. J. Microbiol., 16, 1123–1129, 1970.

Lin, Y. S., Lipp, J. S., Yoshinaga, M. Y., Lin, S. H., Elvert, M., and Hinrichs, K. U.: Intramolecular stable carbon isotopic analysis of archaeal glycosyl tetraether lipids, Rapid Commun. Mass Spectrom., 24, 2817–2826, doi:10.1002/rcm.4707, 2010.

Lipp, J. S., Morono, Y., Inagaki, F., and Hinrichs, K.-U.: Significant contribution of Archaea to 15 extant biomass in marine subsurface sediments, Nature, 454, 991–994, doi:10.1038/nature07174, 2008.

Lipp, J. S., Liu, X. L., and Hinrichs, K. U.: Structural diversity and fate of intact polar lipids in marine sediments, Geochim. Cosmochim. Ac., 73, A771–A771, 2009.

Lunau, M., Lemke, A., Walther, K., Martens-Habbena, W., and Simon, M.: An improved method for counting bacteria from sediments and turbid environments by epifluorescence microscopy, Environ. Microbiol., 7, 961–968, 2005.

Muyzer, G., Dewaal, E. C., and Uitterlinden, A. G.: Profiling of complex microbial-populations by denaturing gradient gel-electrophoresis analysis of polymerase chain reaction-amplified

genes-coding for 16S ribosomal RNA, Appl. Environ. Microbiol., 59, 695–700, 1993.

Muyzer, G., Teske, A., Wirsen, C. O., and Jannasch, H. W.: Phylogenetic relationships of Thiomicrospira species and their identification in deep-sea hydrothermal vent samples by denaturing gradient gel-electrophoresis of 16S rDNA fragments, Arch. Microbiol., 164, 165–172, 1995.

Oremland, R. S. and Taylor, B. F.: Diurnal fluctuations of O_2, N_2 and CH_4 in rhizosphere of Thalassia testundinum, Limnol. Oceanogr., 22, 566–570, 1977.

Ravenschlag, K., Sahm, K., Knoblauch, C., Jørgensen, B. B., and Amann, R.: Community structure, cellular rRNA content, and activity of sulfate-reducing bacteria in marine arctic sediments, Appl. Environ. Microbiol., 66, 3592–3602, doi:10.1128/aem.66.8.3592-3602.2000, 2000.

Rossel, P. E., Lipp, J. S., Fredricks, H. F., Arnds, J., Boetius, A., Elvert, M., and Hinrichs, K. U.: Intact polar lipids of anaerobic methanotrophic archaea and associated bacteria, Org. Geochem., 39, 992–999, doi:10.1016/j.orggeochem.2008.02.021, 2008.

Rütters, H., Sass, H., Cypionka, H., and Rullkötter, J.: Monoalkylether phosphoslipids in the sulfate-reducing bacteria Desufosarcina variablis and Desulforhabus amnigenus, Arch. Microbiol., 176, 435–442, 2001.

Sanyal, S. and Menon, A. K.: Flipping Lipids: Why an Whats the Reason for?, ACS Chem. Biol., 4, 895–909, doi:10.1021/cb900163d, 2009.

Schippers, A., Neretin, L. N., Kallmeyer, J., Ferdelman, T. G., Cragg, B. A., Parkes, R. J., and Jørgensen, B. B.: Prokaryotic cells of the deep sub-seafloor biosphere identified as living bacteria, Nature, 433, 861–864, 2005.

Schouten, S., Middelburg, J. J., Hopmans, E. C., and Sinninghe Damsté, J. S.: Fossilization and degradation of intact polar lipids in deep subsurface sediments: A theoretical approach, Geochim. Cosmochim. Ac., 74, 3806 pp., 2010.

Sherr, E. B. and Sherr, B. F.: Heterotrophic dinoflagellates: a significant component of micro-zooplankton biomass and major grazers of diatoms in the sea, Mar. Ecol.-Prog. Ser., 352, 187–197, doi:10.3354/meps07161, 2007.

Sinninghe Damsté, J. S., Rijpstra, W. I. C., Geenevasen, J. A. J., Strous, M., and Jetten, M. S. M.: Structural identification of ladderane and other membrane lipids of plancto-mycetes capable of anaerobic ammonium oxidation (anammox), FEBS J., 272, 4270–4283, doi:10.1111/j.1742-4658.2005.04842.x, 2005.

Sprott, G. D., Larocque, S., Cadotte, N., Dicaire, C. J., McGee, M., and Brisson, J. R.: Novel

polar lipids of halophilic eubacterium Planococcus H8 and archaeon Haloferax volcanii, BBA-Mol. Cell Biol. L., 1633, 179 pp., 2003.

Sturt, H. F., Summons, R. E., Smith, K., Elvert, M., and Hinrichs, K. U.: Intact polar membrane lipids in prokaryotes and sediments deciphered by high-performance liquid chromatography/electrospray ionization multistage mass spectrometry - new biomarkers for biogeochemistry and microbial ecology, Rapid Commun. Mass Spectrom., 18, 617–628, 2004.

Süß, J., Engelen, B., Cypionka, H., and Sass, H.: Quantitative analysis of bacterial communities from Mediterranean sapropels based on cultivation-dependent methods, FEMS Microbiol. Ecol., 51, 109–121, 2004.

Takano, Y., Chikaraishi, Y., Ogawa, N. O., Nomaki, H., Morono, Y., Inagaki, F., Kitazato, H., Hinrichs, K. U., and Ohkouchi, N.: Sedimentary membrane lipids recycled by deep-sea benthic archaea, Nat. Geosci., 3, 858–861, doi:10.1038/ngeo983, 2010.

White, D. C., Davis, W. M., Nickels, J. S., King, J. D., and Bobbie, R. J.: Determination of the sedimentary microbial biomass by extractable lipid phosphate, Oecologia, 40, 51–62, 1979.

Wilms, R., Sass, H., Kopke, B., Koster, J., Cypionka, H., and Engelen, B.: Specific Bacterial, Archaeal, and Eukaryotic Communities in Tidal-Flat Sediments along a Vertical Profile of Several Meters, Appl. Environ. Microbiol., 72, 2756–2764, doi:10.1128/aem.72.4.2756-2764.2006, 2006.

Wilms, R., Sass, H., Köpke, B., Cypionka, H., and Engelen, B.: Methane and sulfate profiles within the subsurface of a tidal flat are reflected by the distribution of sulfate-reducing bacteria and methanogenic archaea, FEMS Microbiol. Ecol., 59, 611–621, 2007.

Wuchter, C., Abbas, B., Coolen, M. J. L., Herfort, L., van Bleijswijk, J., Timmers, P., Strous, M., Teira, E., Herndl, G. J., Middelburg, J. J., Schouten, S., and Sinninghe Damsté, J. S.: Archaeal nitrification in the ocean, Proc. Natl. Acad. Sci. U.S.A., 104, 5704–5704, doi:10.1073/pnas.0701630104, 2007.

Zink, K. G., Wilkes, H., Disko, U., Elvert, M., and Horsfield, B.: Intact phospholipids – microbial "life markers" in marine deep subsurface sediments, Org. Geochem., 34, 755–769, 2003.

Core lipids   Head groups

A

$R_1, R_2 = CH_3, C_2H_5, C_3H_7$

PE   PS

PC   PI
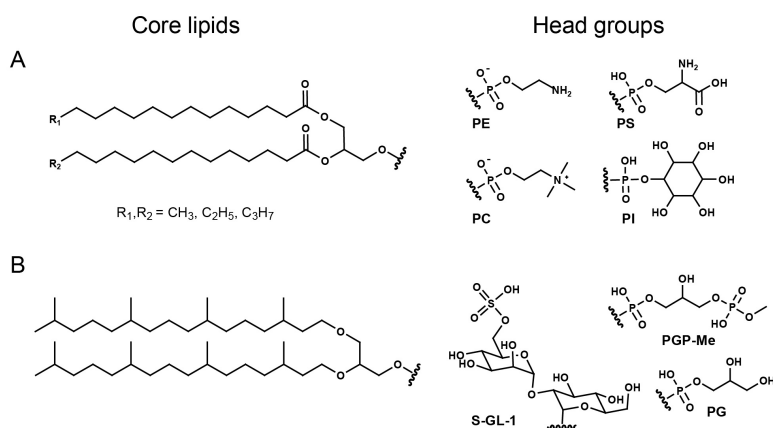
B

S-GL-1   PGP-Me

PG

Fig. 1. Chemical structures of IPLs characteristic for the two organisms used in this study: **(A)** diacylglycerol ester-bound core lipids of *Saccharomyces cerevisiae* bound to: phosphatidylethanolamine (PE), phosphatidylcholine (PC), phosphatidylinositol (PI) and phosphatydylserine (PS); **(B)** isoprenoid ether-bound core lipids of *Haloferax volcanii* bound to: archaetidylglycerol (PG-Ar), archaetidylglycerol methylphosphate (PGP-Me) and sulfono diglyco diacylglycerol S-GL-1 (nomenclature according to Sprott et al., 2003).
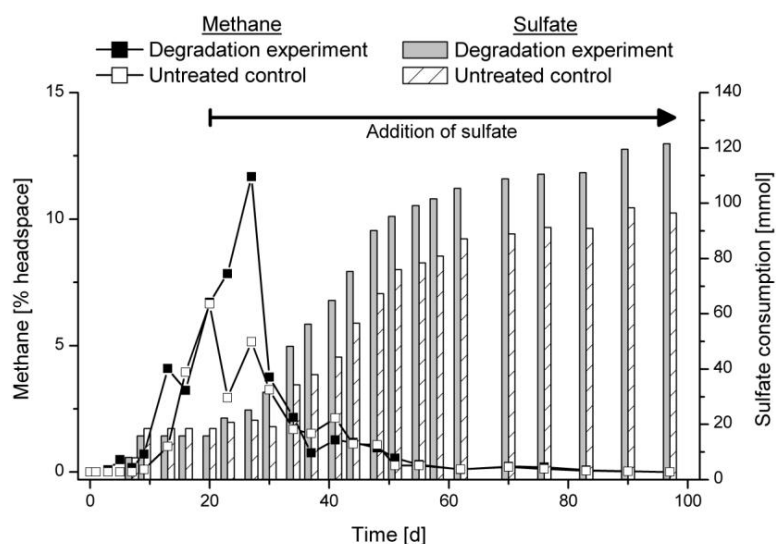
Fig. 2. Sulfate consumption and methane production in the degradation experiment and the untreated control. Sulfate consumption for each time point was calculated by addition of measured day-to-day losses. Methane concentrations are given in percentage of incubation vessel headspace. After day 20 sulfate was refilled when the concentration decreased below 10 mM as indicated by the arrow.
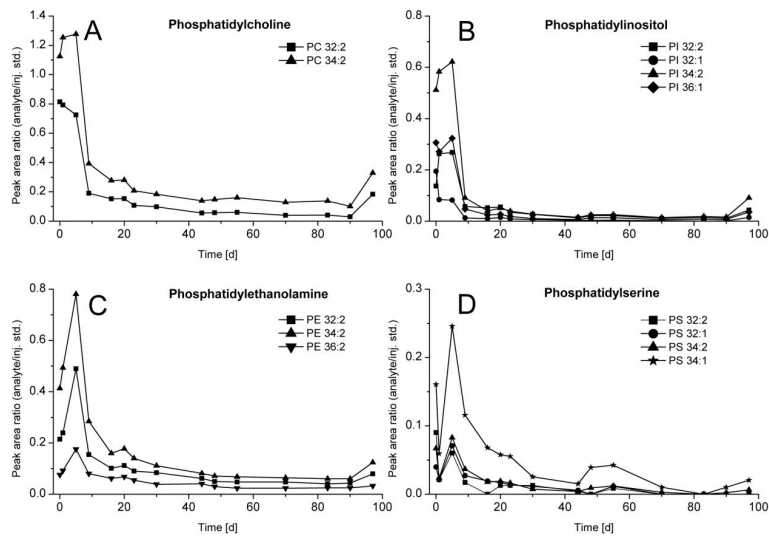
Fig. 3. Relative concentrations of ester-bound IPLs with different head groups in the degradation experiment vs. time in days. Core lipid structures are given as sum of fatty acids (e.g. 32:2) where 32 represents the number of carbon atoms and 2 represents the number of double bonds in the core lipid structure.
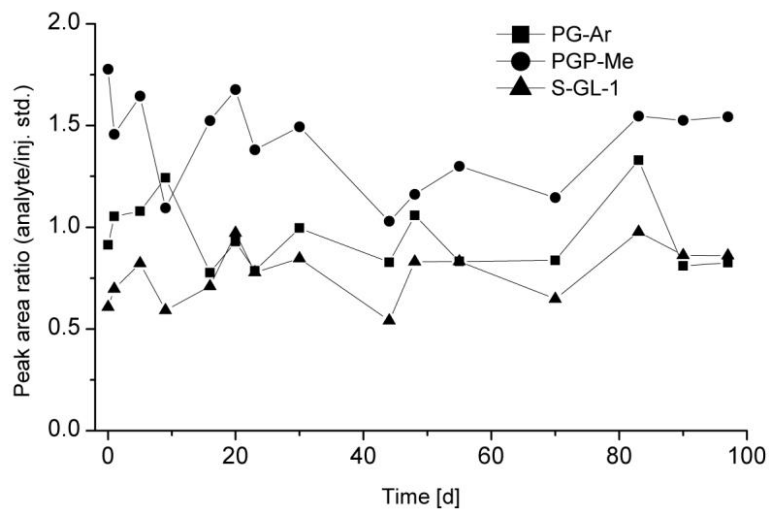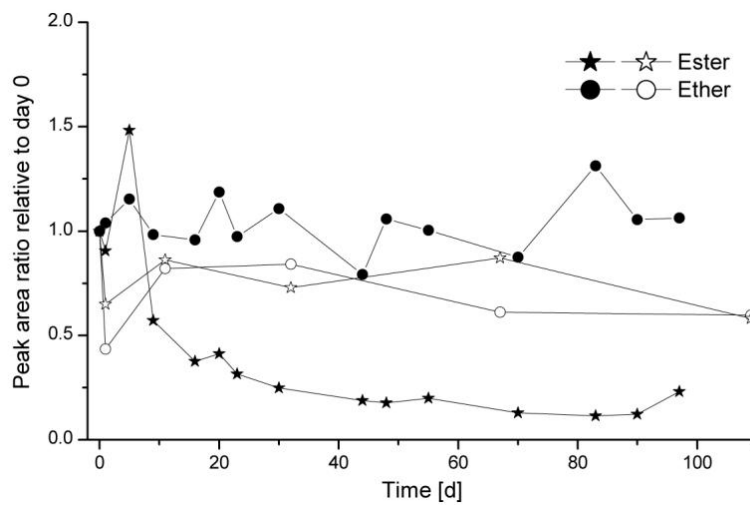
3315

Fig. 4. Relative concentrations of ether-bound IPLs with different head groups in the degradation experiment vs. time in days. Abbreviations: archaetidylglycerol (PG-Ar), archaetidylglycerol methylphosphate (PGP-Me), and sulfono diglyco diacylglycerol S-GL-1 (according to Sprott et al., 2003).

Fig. 5. Sum of ester- and ether-bound IPLs in the degradation experiment and the abiotic control given as relative concentrations relative to day 0. Closed symbols: degradation experiment; open symbols: untreated control.
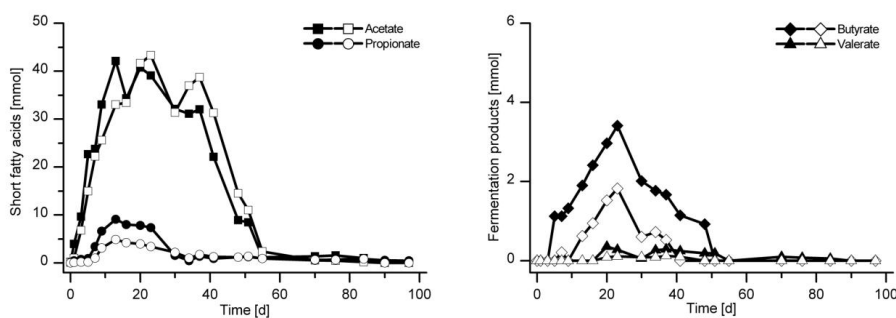
Fig. 6. Pore water concentrations of acetate, propionate, butyrate and valerate in mmol vs. time in days. Closed symbols: degradation experiment; open symbols: untreated control.
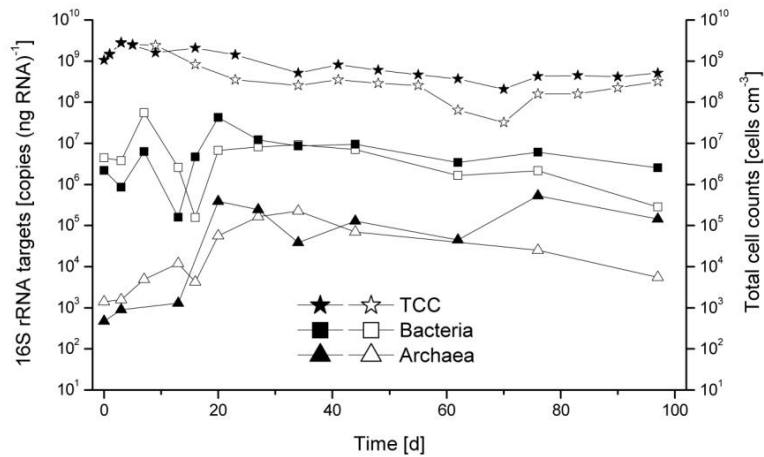
Fig. 7. Bacterial and archaeal 16S rRNA copies and total cell numbers (TCC) in the course of the experiment. The number of bacterial and archaeal 16S rRNA targets are given in copies per ng of extracted RNA, whereas the total cell counts are given in cells per cm^3 sediment. Closed symbols: degradation experiment; open symbols: untreated control.
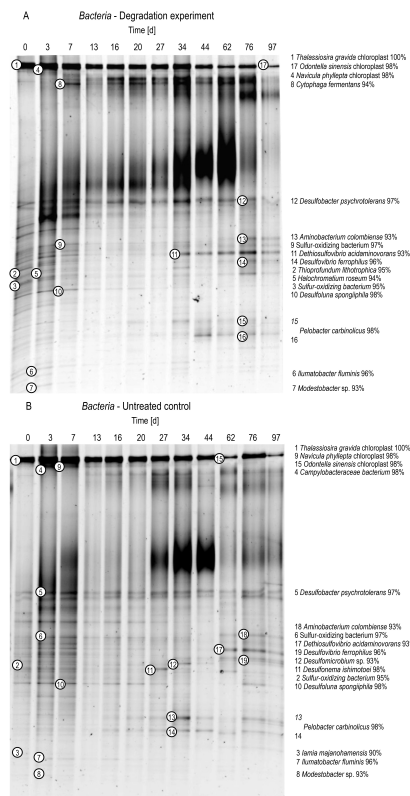
Fig. 8. DGGE community profiles of *Bacteria* and closest cultivated relatives of the sequenced DGGE bands with similarity in % compared to data from the EMBL database. **(A)** degradation experiment **(B)** untreated control.

A   *Archaea* - Degradation experiment

Time [d]

| 0 | 3 | 7 | 13 | 16 | 20 | 27 | 34 | 44 | 62 | 76 | 97 |

21 *Methanogenium frigidum* 97%
22 *Methanogenium frigidum* 97%
23 *Methanogenium marinum* 98%
20 *Haloferax volcanii* 99%
24 *Methanogenium frigidum* 97%

25 *Methanogenium frigidum* 98%

26 *Methanogenium marinum* 98%

B   *Archaea* - Untreated control

Time [d]

| 0 | 3 | 7 | 13 | 16 | 20 | 27 | 34 | 44 | 62 | 76 |

17 *Methanogenium frigidum* 97%
18 *Methanogenium frigidum* 97%
19 *Methanogenium marinum* 98%

20 *Methanogenium frigidum* 97%

21 *Methanogenium frigidum* 97%
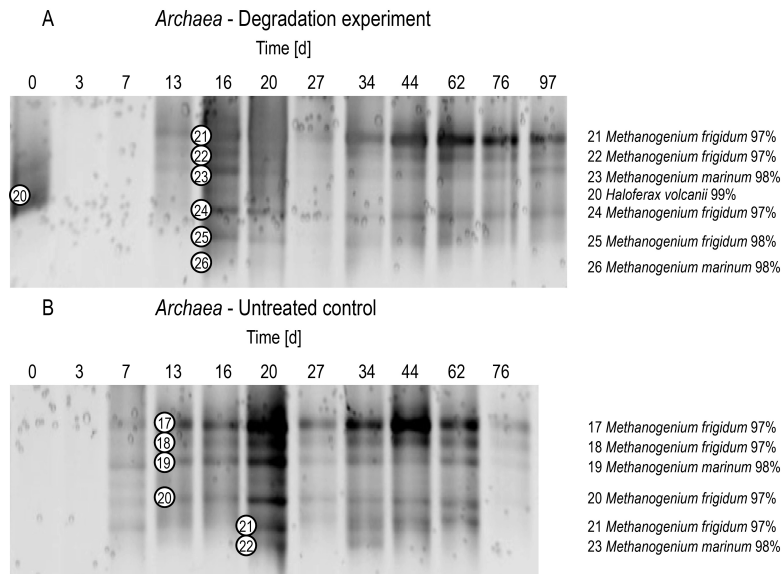23 *Methanogenium marinum* 98%

Fig. 9. DGGE community profiles of *Archaea* and closest cultivated relatives of the sequenced DGGE bands with similarity in % compared to data from the EMBL database. **(A)** degradation experiment **(B)** untreated control.

3321